Biomedical engineering

Stimulation of a myelinated nerve axon by electromagnetic induction

P. J. Basser B. J. Roth

Biomedical Engineering & Instrumentation Program, National Center of Research Resources, National Institutes of Health, Building 13, Room 3W13, Bethesda, MD 20892, USA

Abstract—*A model of electromagnetic stimulation predicts the transmembrane potential distribution along a myelinated nerve axon and the volume of stimulated tissue within a limb. Threshold stimulus strength is shown to be inversely proportional to the square of the axon diameter. It is inversely proportional to pulse duration for short pulses and independent of pulse duration for long ones. These results are also predicted by dimensional analysis. Two dimensionless numbers, S_{em}, the ratio of the induced transmembrane potential to the axon's threshold potential, and τ_c/τ, the ratio of the pulse duration to the membrane time constant, summarise the dependence of threshold stimulus strength on pulse duration and axon diameter.*

Keywords—*Electromagnetic induction, Magnetic stimulation, Mathematical model, Peripheral nerve, Scaling laws, Threshold*

Med. & Biol. Eng. & Comput., 1991, 29, 261–268

1 Introduction

OUR GOAL is to explain the remarkable observation that myelinated axons can be stimulated by electromagnetic induction (BICKFORD and FREMMING, 1965; POLSON *et al.* 1982). It is possible to excite a neuron by passing a time-varying current through a wire coil (Fig. 1). Magnetic stimulation, as this is sometimes called, is noninvasive and relatively painless; it is useful in diagnosing neurological disorders such as multiple sclerosis, and for evoking motor responses (HALLETT and COHEN, 1989). Although commonly used for transcranial activation of the cortex, electromagnetic stimulation has not gained wide acceptance for peripheral nerve stimulation, in part, because of uncertainty in the site of excitation (EVANS *et al.* 1988; CHOKROVERTY, 1989).

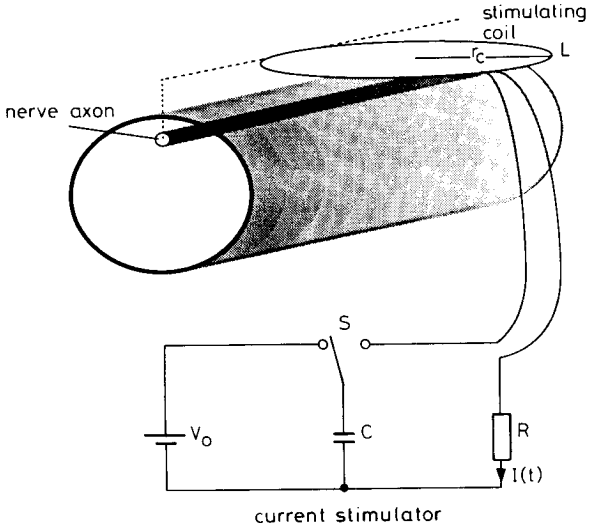

Fig. 1 *Schematic diagram of the cylindrical limb, nerve axon and stimulating circuit. The coil radius r_c is 4·5 cm and the limb radius is 3 cm. When S is switched to the left, the capacitor C charges to a voltage V_0. When S is to the right, the capacitor discharges through a resistance R and inductance L, creating the current pulse $I(t)$ in the coil*

In this paper we present a mathematical model of electromagnetic stimulation of a mammalian peripheral nerve axon within a limb. We calculate the electric field induced within a cylindrical volume conductor and the resulting transmembrane potential along an axon. This model predicts the location of the volume of stimulation within a limb as well as the dependence of threshold stimulus strength on pulse duration and axon diameter. Finally, we derive a simple relationship between the dimensionless stimulus strength and pulse duration which concisely summarises the scaling laws governing the threshold response of the axon.

2 Methods

This description of electromagnetic stimulation of an axon consists of three parts. The current in the stimulating coil is predicted by an *RLC* circuit model. The electric field induced in a cylindrical limb is calculated using Maxwell's equations (ROTH *et al.*, 1990). The distribution of transmembrane potential along the axon is determined from a cable model. The coupling between the induced electric field and the transmembrane potential appears as a single term in the cable equation, a term that we previously derived to describe stimulation of unmyelinated axons (ROTH and BASSER, 1990). To represent a myelinated axon, we use a cable model whose nodal membrane dynamics were measured by CHIU *et al.* (1979), and anatomical scaling relationships derived by RUSHTON (1951) for axons with different diameters.

First received 18th April and in final form 12th July 1990

2.1 *The current pulse waveform*

In most commercial electromagnetic stimulators, a current pulse $I(t)$ is generated by discharging a capacitor C whose initial voltage is V_0 through a coil having resistance R and inductance L (Fig. 1). If the RLC circuit is overdamped, $dI(t)/dt$ is given by

$$\frac{dI(t)}{dt} = \frac{V_0}{L} e^{-\omega_1 t}\left(\cosh(\omega_2 t) - \frac{\omega_1}{\omega_2}\sinh(\omega_2 t)\right) \quad (1)$$

where the frequencies ω_1 and ω_2 are

$$\omega_1 = \frac{R}{2L} \quad \text{and} \quad \omega_2 = \sqrt{\left(\frac{R}{2L}\right)^2 - \frac{1}{LC}} \quad (2)$$

Table 1 contains the values of R, L and C used in these calculations. They approximate the current waveform of an existing magnetic stimulator (BARKER *et al.*, 1985).

Table 1 Values used in the models

Current stimulator model:		
R	stimulating circuit resistance	0·47 Ω
L	stimulating coil inductance	20 μH
C	stimulating circuit capacitance	3100 μF
V_0	voltage across capacitor plates	2000 V
Physical variables:		
x	distance along the axon axis	cm
t	time	ms
$V(x, t)$	transmembrane potential	mV
$\varepsilon_x(x, t)$	total electric field along axon axis	mV cm^{-1}
$I(t)$	stimulating coil current	A
Axon model:		
E_{Na}	sodium Nernst potential @ 37°C	35·35 mV
E_L	leakage Nernst potential @ 37°C	−80·01 mV
g_{Na}	sodium conductance	1445 mS cm^{-2}
g_L	leakage conductance	128 mS cm^{-2}
c_n	nodal capacitance	2·5 μF cm^{-2}
ρ_a	resistivity of axoplasm	5·47 × 10^{-2} kΩ cm
ρ_{mye}	resistivity of myelin	7·4 × 10^5 kΩ cm
κ	dielectric constant of myelin	7
ε_0	permittivity of a vacuum	8·85 × 10^{-8} μF cm^{-1}
δ	width of node of Ranvier	1·5 × 10^{-4} cm

The induced electric field within the limb has the same time course as $dI(t)/dt$ (ROTH, *et al.*, 1990). Accordingly, we define the stimulus strength so that it is proportional to the maximum rate of change of the current in the coil, V_0/L. Furthermore, the stimulus duration τ_c is defined as the elapsed time until the first zero-crossing of $dI(t)/dt$. For the overdamped RLC circuit given in eqns. 1 and 2, the stimulus duration is

$$\tau_c = \frac{1}{2\omega_2}\ln\left(\frac{\omega_1 + \omega_2}{\omega_1 - \omega_2}\right) \quad (3)$$

Figs. 2*a* and *b* show $I(t)$ and $dI(t)/dt$, respectively, as functions of time for the stimulator described by eqn. 1 and the parameters given in Table 1. The stimulus duration τ_c is also shown in both figures.

2.2 *The electric field induced in a cylindrical limb*

The electric field distribution ε induced in a cylindrical limb depends on the coil current, geometry and its orientation with respect to the limb. It is computed by adding the electric field due to electromagnetic induction E_A and the electric field due to the induced charge distribution at the air/tissue interface E_ϕ (ROTH *et al.*, 1990). The former is calculated by approximating the circular stimulating coil as a polygon and then summing the induced electric field produced by each line segment (COHEN *et al.*, 1990*a*). The latter is found by solving Laplace's equation in a homogeneous, cylindrical volume conductor of radius 3 cm, using

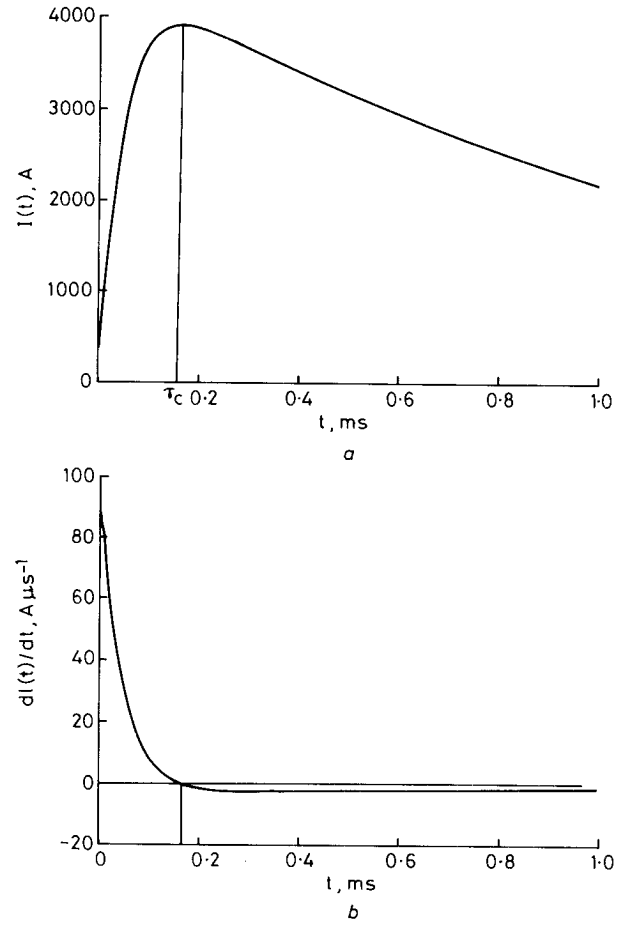

Fig. 2 *(a) Current flowing in the stimulating coil $I(t)$ and (b) its time derivative $dI(t)/dt$ as functions of time. The rate of change of current is positive until the current reaches its maximum value at $t = \tau_c$. Stimulus strength is proportional to $dI(0)/dt$*

a finite-difference technique, with 17 points in the radial direction (separated by 0·1875 cm), 64 in the angular direction (separated by 5·625°) and 129 in the axial direction (separated by 0·1875 cm) (ROTH *et al.*, 1990). For a uniform volume conductor, the electric field is independent of the conductivity of the limb. As shown in Fig. 1, the axon is oriented parallel to the axis of the limb. The 14-turn stimulating coil has a radius r_c of 4·5 cm and lies 0·5 cm above the limb's surface, as shown in Fig. 1. Once the electric field within the limb is known its effect on axon transmembrane potential must be ascertained.

2.3 *Myelinated axon model*

A diagram of a myelinated axon is given in Fig. 3*a*. It consists of segments of active membrane, nodes of Ranvier, that are δ wide and are spaced a distance Λ apart. Each node is modelled as a discrete current source (Fig. 3*b*) that contributes

$$\pi d_i \delta\left(g_{Na} m^2 h(V - E_{Na}) + g_L(V - E_L) + c_n\frac{\partial V}{\partial t}\right) \quad (4)$$

to the membrane current. The gating parameters m and h are governed by the first-order kinetic equations

$$\frac{dm}{dt} = \alpha_m(V)(1 - m) - \beta_m(V)m$$

and

$$\frac{dh}{dt} = \alpha_h(V)(1 - h) - \beta_h(V)h \quad (5)$$

The voltage-dependent rate constants are given (in ms^{-1}) by

$$\alpha_m(V) = \frac{126 + 0{\cdot}363V}{1{\cdot}0 + \exp\left(\frac{-(V + 49)}{5{\cdot}3}\right)}$$

$$\beta_m(V) = \frac{\alpha_m}{\exp\left(\frac{V + 56{\cdot}2}{4{\cdot}17}\right)} \tag{6}$$

$$\alpha_h(V) = \frac{\beta_h}{\exp\left(\frac{V + 74{\cdot}5}{5}\right)}$$

$$\beta_h(V) = \frac{15{\cdot}6}{1 + \exp\left(-\frac{(V + 56)}{10}\right)} \tag{7}$$

where V is the transmembrane potential (in mV). The nodal capacitance per unit area c_n, the sodium conductance per unit area g_{Na}, the leak conductance per unit area g_L, the sodium Nernst potential E_{Na}, the leak Nernst potential E_L and the channel gating kinetics are based on data obtained by CHIU *et al.* (1979) from voltage clamp experiments with rabbit myelinated axons. These values were taken from SWEENEY *et al.* (1987)*, who adjusted CHIU *et al.*'s (1979) results from 14° to 37°C. No potassium current is included in expression 4, which is consistent with the observation by CHIU *et al.* (1979) that potassium channels are absent from the nodal membrane of mammalian myelinated axons.

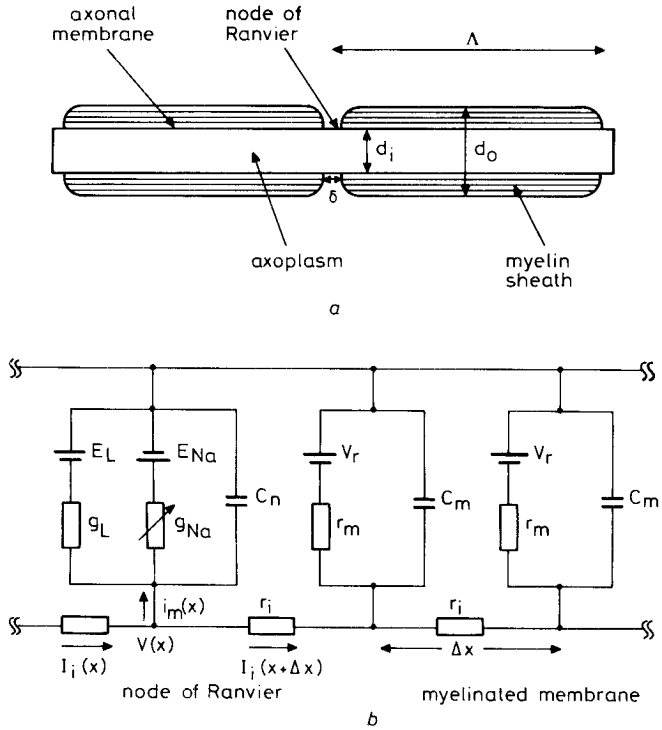

Fig. 3 *(a) Cross-section of a myelinated nerve axon. The axonal membrane contains active regions, nodes of Ranvier, that are joined by passive segments insulated by myelin. Nodes are spaced a distance Λ apart and are δ wide. The axon has an outer diameter of d_o and an inner diameter of d_i. (b) Distributed-circuit model of a myelinated axon. At the node the membrane current per unit length $i_m(x)$ flows through either the nodal membrane capacitance C_n or the sodium or leak channels. Ohm's law relates the axial intracellular current $I_i(x)$ to the intracellular electric field; the equation of continuity relates $I_i(x)$ to the membrane current per unit length $i_m(x)$; The intracellular resistance per unit length is r_i; the extracellular resistance is zero. The capacitance per unit length of the myelin is c_m; the resistance length of the myelin is r_m. E_L and E_{Na} are the leakage and sodium Nernst potentials, respectively; g_L and g_{Na} are the leakage and sodium conductances, respectively. The batteries V_r represent the action of active pumps and channels beneath the myelin that maintain the resting potential of the membrane at −80 mV*

The nodes are joined by lengths of passive axon which are insulated by a myelin sheath (Fig. 3*a*). In the internodal region, the transmembrane potential is governed by a cable equation

$$\lambda_{mye}^2 \frac{\partial^2 V}{\partial x^2} - \tau_{mye} \frac{\partial V}{dt} - (V - V_r) = \lambda_{mye}^2 \frac{\partial \varepsilon_x(x, t)}{\partial x} \tag{8}$$

The space constant of the internodal region λ_{mye} is defined by

$$\lambda_{mye} = d_i \sqrt{\frac{\rho_{mye}}{8\rho_a} \ln\left(\frac{d_o}{d_i}\right)} \tag{9}$$

(FITZHUGH, 1969) and the time constant τ_{mye} by

$$\tau_{mye} = \varepsilon_0 \kappa \rho_{mye} \tag{10}$$

where ρ_{mye} and ρ_a are the resistivities of myelin and axoplasm, respectively, κ is the dielectric constant of myelin, ε_0 is the permittivity of a vacuum, d_o is the outer diameter of the myelin sheath and d_i is the diameter of the axonal membrane. The rest potential V_r is −80 mV; CHIU and RITCHIE (1984) contend that potassium ion channels beneath the myelin sheath maintain a uniform resting potential throughout the internodal region. We also assume that the resistance of the extracellular space is negligible, which may not be valid for axons that are tightly packed in a nerve bundle where a more detailed model may be needed (ALTMAN and PLONSEY, 1988).

The distributed cable equation (eqn. 8) is solved explicitly for the entire axon. At a node, eqns. 4–7 are included as an additional source of transmembrane current; no auxiliary equations are needed as in FITZHUGH (1962) to guarantee that current is continuous at the node.

During electromagnetic stimulation, the axon first fires where the negative gradient of the component of the electric field in the axial direction reaches a maximum. We previously derived a source term of the form $-\lambda^2 \partial \varepsilon_x(x, t)/\partial x$ in the cable equation of an unmyelinated axon which specifies how the induced electric field gives rise to a transmembrane current (ROTH and BASSER, 1990).

Once the electromagnetic source term is prescribed, formal analogies can be drawn between electromagnetic stimulation and stimulation by a microelectrode or extracellular electrodes by comparing their respective dynamic equations. For stimulation with extracellular electrodes, $\partial \varepsilon_x/\partial x$ is replaced by $-\partial^2 V_e/\partial x^2$ in eqn. 8, where V_e is the extracellular potential developed by the electrodes (RATTAY, 1986; 1988). For stimulation with an intracellular microelectrode, $\partial \varepsilon_x/\partial x$ is replaced by $-r_i i_p$ in eqn. 8, where i_p is the inward applied current per unit length and r_i is the resistance per unit length of the axoplasm (PLONSEY, 1969).

* *There are several differences between our work and the abstract by SWEENEY et al. (1987). First, they express the units of g_{Na} and g_L in 'S/cm²'; but to be consistent with CHIU et al. (1979) the same numbers should have been given in 'mS/cm²' (e.g. the correct maximum sodium conductance per unit area is 1445 mS/cm²). Secondly, in the definition of α_m, SWEENEY et al. express the argument of the exponential as '−(V + 49)/53', whereas it should be given as '−(V + 49)/5·3'.*

RUSHTON (1951) postulated three scaling relationships for myelinated axons of different diameters, which have been verified experimentally (GOLDMAN and ALBUS, 1968). First, the distance between nodes varies linearly with axon diameter. Experimental data suggest that the node spacing is about 100 times the myelin outer diameter, although this relationship does not hold for an axon whose diameter is less than 4 μm (RITCHIE, 1982)

$$\frac{L}{d_o} = 100 \tag{11}$$

Secondly, the ratio of the inner and outer diameters of the myelin sheath is constant,

$$\frac{d_i}{d_o} = 0{\cdot}6 \tag{12}$$

Thirdly, the width of the node δ is independent of axon size (FITZHUGH, 1969). We choose $\delta = 1{\cdot}5\,\mu$m (SWEENEY *et al.*, 1987).

The system of nonlinear partial differential equations, eqns. 4–12, is solved numerically on a Cray XMP-24 (ASCL, National Cancer Institute, Frederick, Maryland) using the method of lines—a finite element algorithm (IMSL Scientific Subroutine Library). The membrane is initially at rest, i.e. $V(x, 0) = V_r$; both ends of the axon are assumed to be sealed.

3 Results

Fig. 4 shows a contour plot of the transmembrane potential as a function of the distance x along the axon and the time t after the onset of the stimulus for a axon with an outer diameter of 20 μm. The plane $x = 0$ is perpendicular to the axon and passes through the centre of the coil. The axon is assumed to lie 0·15 cm below the top surface of the limb. After a latency of approximately 0·15 ms, two action potentials develop, propagating in opposite directions with speeds of about 66 m s^{-1}. The origin of stimulation, $x = -2{\cdot}5$ cm, corresponds to the position where $-\partial\varepsilon_x(x,t)/\partial x$ reaches a maximum. Membrane hyperpolarisation is greatest at $x = +2{\cdot}5$ cm where $-\partial\varepsilon_x(x, t)/\partial x$ is a minimum. Although $x = 0$ is the position where $\varepsilon_x(x, t)$ reaches a maximum, $-\partial\varepsilon_x(x, t)/\partial x$ vanishes there. The $V = 0$ contour shows that the travelling wave front rises faster than it falls.

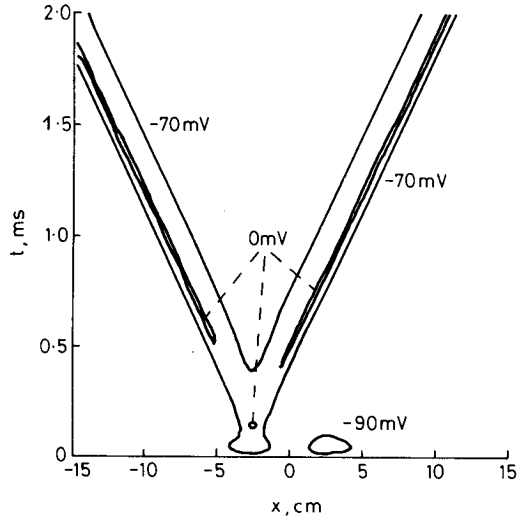

Fig. 4 *Contour plot of the transmembrane potential along a 20 μm axon located 0·15 cm below the surface of the limb, in response to a suprathreshold stimulus ($V_0 = 1600$ V). The origin of stimulation is at $x = -2{\cdot}5$ cm while the latency is approximately 0·15 ms*

We define threshold stimulus strength in the following way: we determine when and where along the axon the stimulus strength $-\partial\varepsilon_x(x, t)/\partial x$ reaches a maximum value (in the previous example at $x = -2{\cdot}5$ cm at $t = 0$). The threshold stimulus strength is the minimum value of this quantity that is sufficient to elicit an action potential. Threshold stimulus strength is determined to within $\pm 0{\cdot}5$ per cent using a binary search algorithm. Stimulation usually occurs when the membrane is depolarised from rest by about 20 mV or to $V = -60$ mV.

For a set of current pulses with the same duration, threshold stimulus strength is proportional to the initial voltage on the capacitor in the stimulating circuit V_0. Fig. 5 shows the predicted relationship between V_0 and the outer diameter of the axon d_o. The axon lies 0·15 cm below the surface of the limb. A regression line was fitted to the data; it was found to have a slope of $-2{\cdot}01$ and a coefficient of correlation of 0·9997. The model predicts that threshold stimulus strength is inversely proportional to the square of the axon diameter.

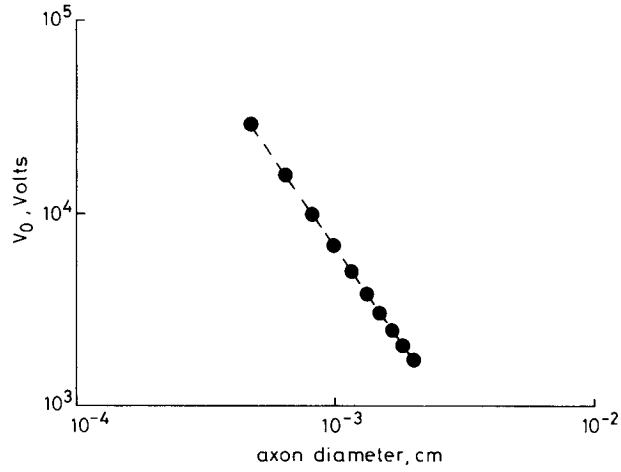

Fig. 5 *Threshold capacitor voltage required to stimulate axons of different diameters. The stimuli have different amplitudes but the same durations. A regression line was fitted to the data; it has a slope of $-2{\cdot}01$ and a coefficient of correlation of 0·9997, indicating that threshold voltage is inversely proportional to the square of the axon diameter ($R = 0{\cdot}47\,\Omega$, $L = 20\,\mu$H, $C = 3100\,\mu$F, axon depth = 0·15 cm)*

The temporal envelope of $-\partial\varepsilon_x(x,t)/\partial x$ also influences whether or not the axon is stimulated. The relationship between threshold stimulus strength and pulse duration τ_c is shown in Fig. 6 for three different axon diameters. Experimentally, τ_c can be varied independently of the stimulus strength by altering R or C. In generating Fig. 6, L was kept constant while R and C were chosen to keep the damping factor of the circuit $(R/2)\sqrt{C/L}$ unchanged, thereby making the set of applied current pulses self-similar. Threshold stimulus strength asymptotically approaches a constant value for long duration pulses and is inversely proportional to duration for short pulses.

It is of great clinical value and scientific interest to determine the regions of excitation within a tissue mass following electromagnetic stimulation. We call this region the 'volume of stimulation' (RATTAY, 1987). It is bounded by surfaces along which $\partial\varepsilon_x(x, y, z, 0)/\partial x = -682$ mV cm^{-2} (Fig. 7*a*). Within the volume of stimulation axons whose outer diameters are 20 μm or larger will be excited. The volume of stimulation has two lobes, one below the circular coil but displaced from its centre and the other oriented almost perpendicular to the plane of the coil. Fig. 7*b* shows transverse sections of the limb in which the volume of stimulation is shown in black. Note that no stimulation

occurs along the transverse plane $x = 0$ because the axial electric field gradient vanishes there by symmetry. If blocking, rather than initiating, nerve conduction was of interest, the regions of tissue hyperpolarisation could be calculated and displayed in an analogous fashion.

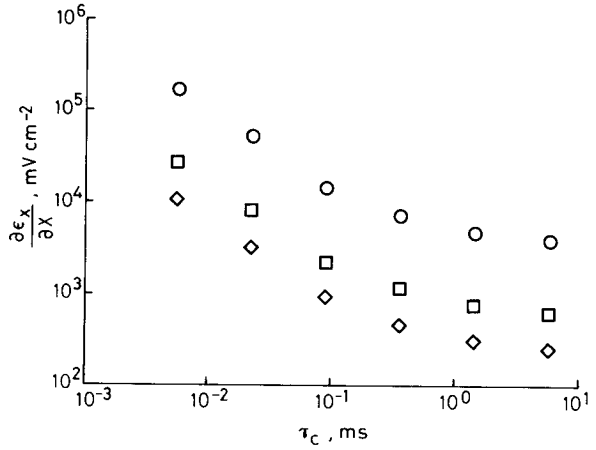

Fig. 6 *Threshold stimulus strength against stimulus duration. This simulation is performed by varying the resistance and capacitance in the stimulating circuit while keeping the damping factor constant. The threshold stimulus strength approaches an asymptote for long duration pulses and is inversely proportional to τ_c for short duration pulses. Smaller diameter axons require larger threshold stimuli*
○ *5 μm* □ *12·5 μm* ◇ *20 μm*

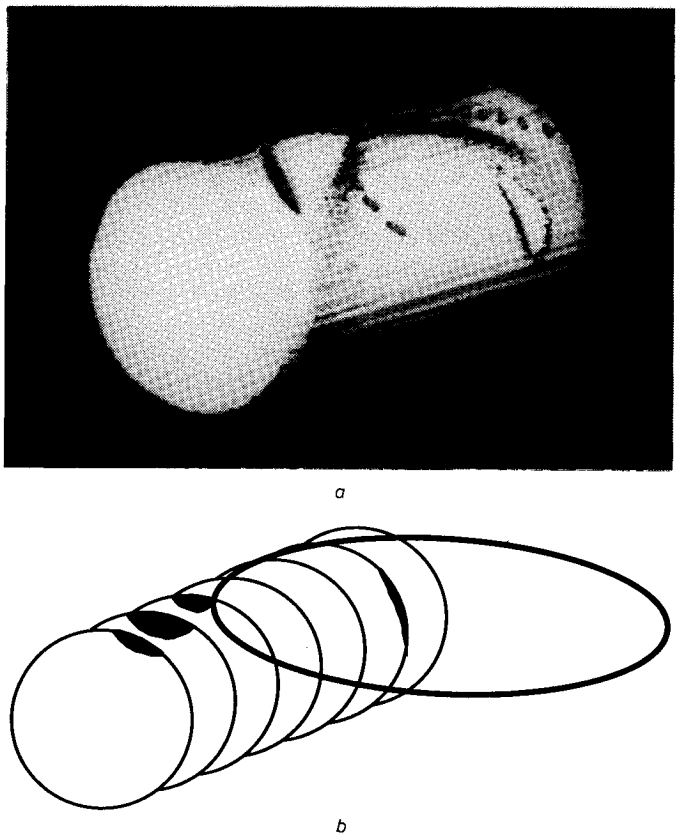

a

b

Fig. 7 *(a) Three-dimensional rendering of the volume of stimulation in a cylindrical limb, produced by a circular coil. The regions in which threshold stimulus strength is greater than 682 mV cm^{-2} are displayed as cavities in this computer-generated figure. An axon that is oriented axially, with a diameter greater than or equal to 20 μm, and passing through one of these cavities is expected to be stimulated. (b) Series of transverse cross-sections of the limb showing the volume of stimulation (black). Successive slices are separated by 1·5 cm and the coil radius is 4·5 cm*

In Figs. 7*a* and *b*, the current flows clockwise in the coil (viewed from above). If the current polarity were reversed, the lobes of the volume of stimulation would be reflected across the plane $x = 0$. With a reversal of polarity we also expect a difference in the arrival time of action potentials (or EMGs) at a distance electrode (ROTH and BASSER, 1990). For a 20 μm axon 0·15 cm below the limb surface, we predict a time difference of approximately 0·8 ms, which is calculated by dividing the distance between the extrema in $\partial \varepsilon_x / \partial x$ by the conduction velocity of the action potential.

4 Discussion

To explain relationships between threshold stimulus strength, axon diameter and pulse duration, we simplify our model of the axon to include only essential elements. First, we consider the passive, subthreshold response of the axon by ignoring the sodium current. This approximation is justified since we consider where and when an action potential fires, not the subsequent dynamic behaviour of the axon once it is stimulated. Secondly, the distance over which the potential varies is in the order of the coil diameter, which is large compared to the separation between nodes of Ranvier. Therefore, the equations describing an axon with discrete, nodal current sources can be simplified to an equation of a uniform axon. This equivalent representation of the cable equation, suggested by ANDRIETTI and BERNARDINI (1984), can be achieved using the method of multiple scales (e.g., KELLER 1977; 1980). This method reduces to averaging the membrane impedances over the nodal and internodal regions. With these assumptions and RUSHTON's (1951) scaling laws for axons of different diameters (eqns. 11 and 12), we derive a simplified subthreshold cable equation for electromagnetic stimulation

$$\lambda^2 \frac{\partial^2 V}{\partial x^2} - \tau \frac{\partial V}{\partial t} - (V - V_r) = \lambda^2 \frac{\partial \varepsilon_x(x, t)}{\partial x} \tag{13}$$

where the length and time constants λ and τ for the equivalent axon are

$$\lambda = d_o \sqrt{\frac{15}{\rho_a g_L \delta + 652 \frac{\rho_a}{\rho_{mye}}}} \tag{14}$$

and

$$\tau = \frac{c_n + 652 \frac{\kappa \varepsilon_o}{\delta}}{g_L + 652 \frac{1}{\rho_{mye} \delta}} \tag{15}$$

Using the parameters in Table 1, $\tau = 0{\cdot}0388$ ms and $\lambda = 117 d_o$ or $1{\cdot}17 \Lambda$. For a 20 μm axon, the length constant is 0·234 cm.

The cable equation, eqn. 13, describes many salient features of electromagnetic stimulation of axons. By rescaling the variables in this equation, we estimate the relative importance of each of its terms and derive quantitative relationships between its parameters. The axial coordinate x is normalised by the radius of the stimulating coil r_c, which is the relevant length scale of the stimulation that is imposed upon the axon

$$x = \frac{x}{r_c} \tag{16}$$

As x and r_c both have units of cm, the new variable x is dimensionless. Similarly, time t is normalised by the stimulus duration τ_c

$$t = \frac{t}{\tau_c} \tag{17}$$

The axial electric field gradient $(\partial\varepsilon_x(x, t)/\partial x)$ is scaled by its extreme value $(\partial\varepsilon_x/\partial x_{max})$ with respect to both space and time

$$\frac{\partial\varepsilon_x(x, t)}{\partial x} = \frac{\dfrac{\partial\varepsilon_x(x, t)}{\partial x}}{\dfrac{\partial\varepsilon_x}{\partial x_{max}}} \tag{18}$$

and the deviation of the transmembrane potential from its resting value is normalised by the change in potential required to elicit an action potential—its threshold potential V_T,

$$V = \frac{V - V_r}{V_T} \tag{19}$$

We substitute these normalised variables into the cable equation to obtain

$$\left(\frac{\lambda}{r_c}\right)^2 \frac{\partial^2 V}{\partial x^2} - \left(\frac{\tau}{\tau_c}\right)\frac{\partial V}{\partial t} - V = \left(\frac{\lambda^2}{V_T}\left(\frac{\partial\varepsilon_x}{\partial x}\right)_{max}\right)\frac{\partial\varepsilon_x(x, t)}{\partial x} \tag{20}$$

The behaviour of this normalised cable equation is determined by the three dimensionless parameters enclosed in parentheses. In most applications of electromagnetic stimulation, the square of the ratio of the length constant and the coil radius is in the order of 10^{-3}, so that the first term on the left hand side of eqn. 20 is negligible. Therefore, the transmembrane potential is determined by the two remaining dimensionless parameters in eqn. 20. We define T as the ratio of the membrane time constant and stimulus duration; we call the dimensionless parameter on the right hand side of eqn. 20 the electromagnetic stimulation number S_{em}

$$S_{em} = \frac{\lambda^2}{V_T}\frac{\partial\varepsilon_x}{\partial x^{max}} \tag{21}$$

For a stimulus whose duration is long with respect to the axon time constant (i.e., a rheobase stimulus $\tau \ll \tau_c$) S_{em} is the ratio of the magnitude of the induced transmembrane potential $\lambda^2(\partial\varepsilon_x/\partial x^{max})$ and the axon's intrinsic threshold potential V_T. S_{em} is less than one for subthreshold stimuli and greater than one for suprathreshold stimuli. We can use this threshold condition, $S_{em} = 1$, to make an *a priori* estimate of the magnitude of the minimum applied electric field gradient sufficient to stimulate a 20 μm myelinated axon ($\lambda = 0{\cdot}234$ cm, $V_T = 20$ mV, $S_{em} = 1$)

$$\left(\frac{\partial\varepsilon_x(x, t)}{\partial x}\right)_{max} \simeq \frac{V_T}{\lambda^2} = 365\ \frac{\text{mV}}{\text{cm}^2} \tag{22}$$

This estimated value is within a factor of two of the threshold stimulus strength calculated numerically for a 20 μm axon, 682 mV cm^{-2}.

Using eqn. 20, we can also explain why the threshold stimulus strength is inversely proportional to the outer diameter of the axon, as shown in Fig. 5. The substitution of the definition of the length constant, eqn. 14, into the expression for S_{em} and the regrouping of terms gives

$$S_{em} = \left\{\frac{15}{\rho_a g_L \delta + 652\dfrac{\rho_a}{\rho_{mye}}}\right\}\left(\frac{d_o^2}{V_T}\left(\frac{\partial\varepsilon_x}{\partial x}\right)_{max}\right) \tag{23}$$

If we assume that the physical properties of myelin and axoplasm, and the node width, are all independent of axon diameter (FITZHUGH, 1969), the term within brackets on the right hand side of eqn. 23 must be constant, i.e. independent of axon size (using our parameters it equals 14 400). Rushton's 'principle of corresponding states' (i.e. corresponding parts of myelinated axons of different diameter are equipotential) implies that the threshold potential V_T also does not vary with axon size (RUSHTON, 1951). Therefore, for a constant stimulus duration, we conclude that

$$\left(\frac{\partial\varepsilon_x}{\partial x}\right)_{max} \propto \frac{1}{d_o^2} \tag{24}$$

We again use the nondimensional cable equation to explain the strength/duration data shown in Fig. 6. We neglect the term in eqn. 20 containing the small parameter λ/r_c and evaluate the cable equation at the position where $\partial\varepsilon_x/\partial x$ is maximum. Recalling that $\partial\varepsilon_x/\partial x$ is proportional to $dI(t)/dt$, we obtain

$$-T\frac{\partial V}{\partial t} - V = S_{em}e^{-\tau_c\omega_1 t} \times \left(\cosh(\tau_c\omega_2 t) - \frac{\omega_1}{\omega_2}\sinh(\tau_c\omega_2 t)\right) \tag{25}$$

Given that the transmembrane potential is initially at rest ($V(0) = 0$), we can solve this equation analytically, finding

$$V(t) = \frac{-S_{em}}{\beta - \alpha}\left\{\left[\frac{\alpha}{1 - T\alpha} - \frac{\beta}{1 - T\beta}\right] \times e^{-t/T} - \frac{\alpha}{1 - T\alpha}e^{-\alpha t} + \frac{\beta}{1 - T\beta}e^{-\beta t}\right\} \tag{26}$$

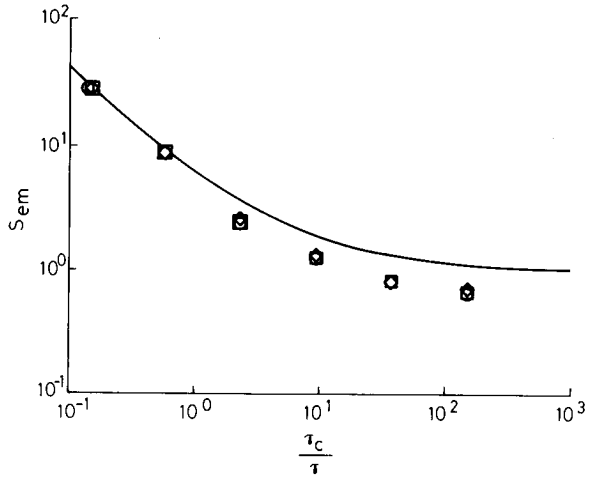

Fig. 8 *Plot of the dimensionless electromagnetic stimulation number S_{em} at threshold against the normalised pulse period τ_c/τ computed numerically. Superimposed is the solution to the homogenised, passive cable model eqn. 26. This curve summarises the results of many numerical experiments in which nerve diameter and pulse duration are varied and establishes the utility of the homogenised model for describing near threshold events in electromagnetic stimulation*
○ 5 μm □ 12·5 μm ◇ 20 μm

where two new dimensionless parameters, α and β, are related to the time course of the current pulse $\alpha = \tau_c(\omega_1 - \omega_2)$ and $\beta = \tau_c(\omega_1 + \omega_2)$. Varying α and β to keep the damping factor constant, we determine the value of S_{em} required for $V(t)$ to reach a maximum value of 1 using eqn. 26 and evaluate the dimensionless duration, $\tau_c/\tau = 1/T$, using eqn. 3. These equations predict the strength/duration curve shown as a solid curve in Fig. 8. Juxtaposed are the numerical data obtained using the full nonlinear model. The curve does not have the classical $1/(1 - e^{-1/T})$ form which is appropriate for electrical stimulation with rectangular current pulses (GEDDES, 1988)—the transition from long to short durations is wider. Good agreement is seen between the theoretical and numerical results. Thus, the simplified model concisely summarises the results of many numerical experiments.

This model of electromagnetic stimulation depends on several assumptions which must still be examined with great care. For instance, we assume the limb is a homogeneous cylindrical volume conductor containing a homogeneous axon oriented parallel to the axis of the limb. We also assume that the induced transmembrane potential depends only on the axial position along the axon and does not vary over the axon cross-section. The validity of these assumptions can only be ascertained by a more detailed three-dimensional analysis. For now, we must be cautious in using this model to interpret *in vivo* experimental results.

This model could be used to address any interaction of low-frequency electromagnetic fields with electrically active tissue. For instance, in magnetic resonance imaging the rapidly varing gradient magnetic fields can induce electric fields in the body that give rise to sensory stimulation (COHEN *et al.*, 1990*b*). Another application is in health physics. The model can be used to calculate the induced electric fields caused by high-voltage power lines.

Finally, as an aside, if the axon were to follow a sinuous path within the tissue or be oriented skew to the plane of the coil, it is still possible to calculate the induced electric field in the direction of the axon. The trajectory of the axon can be represented as a space curve that is parameterised by its arc-length s i.e. $\boldsymbol{r} = \boldsymbol{r}(s)$, where $\boldsymbol{r}$ is the displacement vector which points to an element of the axon $\boldsymbol{dr}(s)$. For simplicity, the origin of this co–ordinate system is the same one used to describe the electric field. In eqn. 20, $-(\partial\varepsilon_x/\partial x)$ is replaced by

$$-\frac{\partial}{\partial s}\left(\boldsymbol{E}(\boldsymbol{r}(s), t) \cdot \frac{\dfrac{d\boldsymbol{r}(s)}{ds}}{\left|\dfrac{d\boldsymbol{r}(s)}{ds}\right|}\right) \tag{27}$$

5 Conclusion

This model of magnetic stimulation makes several testable predictions about the action of an induced electromagnetic field on an axon. By using Maxwell's equations and a cable equation we have explained why an axon is stimulated by electromagnetic induction—the induced axial electric field gradient causes a depolarising current to flow across the axonal membrane. The origin of stimulation occurs where the negative induced electric field gradient is a maximum along the axon. Relationships between threshold stimulus strength, axon diameter and pulse duration, and the locus of the volume of stimulation, can be used to predict whether an axon will be stimulated electromagnetically.

Acknowledgments—We would like to thank Geoff Sobering for his help in producing Fig. 7. We are also grateful to Drs Mark Hallett and Leonardo Cohen for their encouragement. We wish to thank Ichiji Tasaki for enjoyable discussions and acknowledge the contribution of the National Cancer Institute for allocation of computing time and staff support at the Advanced Scientific Computing Laboratory at the Frederick Cancer Research Facility.

References

ALTMAN, K. W. and PLONSEY, R. (1988) Development of a model for point source electrical fibre bundle stimulation. *Med. & Biol. Eng. & Comput.*, **26,** 466-475.

ANDRIETTI, F. and BERNARDINI, G. (1984) Segmented and 'equivalent' representation of the cable equation. *Biophys. J.*, **46,** 615-623.

BARKER, A. T., JALINOUS, R. and FREESTON, I. L. (1985) Noninvasive magnetic stimulation of human motor cortex. *Lancet*, **1,** 1106-1107.

BICKFORD, R. G. and FREMMING, B. D. (1965) Neuronal stimulation by pulsed magnetic fields in animals and man. Dig. 6th Int. Conf. Med. Electronics Biol. Eng., 112.

CHIU, S. Y., RITCHIE, J. M., ROGART, R. B. and STAGG, D. (1979) A quantitative description of membrane currents in rabbit myelinated nerve. *Lond. J. Physiol.*, **292,** 149-166.

CHIU, S. Y. and RITCHIE, J. M. (1984) On the physiological role of internodal potassium channels and the security of conduction in myelinated nerve fibres. *Proc. R. Soc. Lond. B*, **220,** 415-422.

CHOKROVERTY, S. (1989) Magnetic stimulation of the human peripheral nerves. *Electromyogr. Clin. Neurophysiol.*, **29,** 409-416.

COHEN, L. G., ROTH, B. J., NILSSON, J., DANG, N., PANIZZA, M., BANDINELLI, S., FRIAUF, W. and HALLETT, M. (1990*a*) Effect of coil design on delivery of focal magnetic stimulation. I. Technical considerations. *Electroenceph. Clin. Neutrophysiol.*, **75,** 350-357.

COHEN, M. S., WEISSKOPF, R. O., RZEDZIAN, H. L. and KANTOR, H. L. (1990*b*) Sensory stimulation by time-varying magnetic fields. *Magn. Reson. Med.*, **14,** 409-414.

EVANS, B. A., LITCHY, W. J. and DAUBE, J. R. (1988) The utility of magnetic stimulation for routine peripheral nerve conduction studies. *Muscle & Nerve*, **11,** 1074-1078.

FITZHUGH, R. (1962) Computation of impulse initiation and saltatory conduction in a myelinated nerve fiber. *Biophys. J.*, **2,** 11-21.

FITZHUGH, R. (1969) Mathematical models of excitation and propagation in nerve. In *Biological engineering*. SCHWAN, H. (Ed.), McGraw-Hill, 1-83.

GEDDES, L. A. (1988) Optimal stimulus duration for extracranial cortical stimulation. *Neurosurg.*, **20,** 94-99.

GOLDMAN, L., and ALBUS, J. S. (1968) Computation of impulse conduction in myelinated fibers: theoretical basis of the velocity-diameter relation. *Biophys. J.*, **8,** 596-607.

HALLETT, M. and COHEN, L. G. (1989) Magnetism: a new method for stimulation of nerve and brain. *JAMA*, **262,** 538-541.

KELLER, J. B. (1977) Effective behavior of heterogeneous media, In *Statistical mechanics and statistical methods.* In *Theory and applications.* LANDMAN, U. (Ed.) Plenum Press, New York, 631-644.

KELLER, J. B. (1980) Darcy's law for flow in porous media and the two-space method. In *Nonlinear partial equations.* In *Engineering and applied science*, STERNBERG, R. L., KALINOWSKI, A. J. and PAPADAKIS, J. S. (Eds.) Marcel Dekker, New York, 429-443.

PLONSEY, R. (1969) *Bioelectric phenomena.* McGraw-Hill, New York.

POLSON, M. J. R., BARKER, A. T. and FREESTON, I. L. (1982) Stimulation of nerve trunks with time-varying magnetic fields. *Med. & Biol. Eng. & Comput.*, **20,** 243-244.

RATTAY, F. (1986) Analysis of models for external stimulation of axons. *IEEE Trans.*, **BME-33,** 974-977.

RATTAY, F. (1987) Ways to approximate current-distance relations for electrically stimulated fibers. *J. Theor. Biol.*, **125,** 339-349.

RATTAY, F. (1988) Modeling the excitation of fibers under surface electrodes. *IEEE Trans.*, **BME-35,** 199-202.

RITCHIE, J. M. (1982) On the relation between fibre diameter and conduction velocity in myelinated nerve fibres. *Proc. R. Soc. Lond. B*, **217**, 29-35.

ROTH, B. J. and BASSER, P. J. (1990) A model of the stimulation of a nerve fiber by electromagnetic induction. *IEEE Trans.*, **BME-37**, 588-597.

ROTH, B. J., COHEN, L. G., HALLETT, M., FRIAUF, W. and BASSER, P. J. (1990) A theoretical calculation of the electric field induced by magnetic stimulation of a peripheral nerve. *Muscle & Nerve*, **13**, 734–741.

RUSHTON, W. A. H. (1951) A theory of the effects of fibre size in medullated nerve. *J. Physiol. (London)*, **115**, 101-122.

SWEENEY, J. D., MORTIMER, J. T. and DURAND, D. (1987) Modeling of mammalian myelinated nerve for functional neuromuscular stimulation. In Proc. of the 9th Ann. Conf. of IEEE EMBS, 1577–1578.

Authors' biographies

Peter Basser received his AB degree in Engineering Sciences from Harvard College in 1980; he received his SM and Ph.D. degrees from Harvard University in 1982 and 1986, respectively. He is currently a Senior Staff Fellow at the Biomedical Engineering & Instrumentation Programme at the US National Institutes of Health in Bethesda, Maryland, USA. His research interests include developing continuum models of electromechanochemical conversion in polymer gels, water flow in tissue and electromagnetic stimulation of nerves.

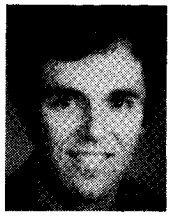

Brad Roth received the BS degree in Physics from the University of Kansas in 1982, and the Ph.D. degree in Physics from Vanderbilt University in 1987. He is presently a Staff Fellow with the Biomedical Engineering & Instrumentation Program at the National Institutes of Health in Bethesda, Maryland, USA. His research interests are in the interaction of electric and magnetic fields with biological tissues, including the electromagnetic stimulation of nerves.